© 2019. Published by The Company of Biologists Ltd | Journal of Experimental Biology (2019) 222, jeb198564. doi:10.1242/jeb.198564

RESEARCH ARTICLE

Severe thermoregulatory deficiencies in mice with a deletion in the titin gene *TTN*

Carissa A. Miyano*, Santiago F. Orezzoli, C. Loren Buck and Kiisa C. Nishikawa

ABSTRACT

Muscular dystrophy with myositis (*mdm*) mice carry a deletion in the N2A region of the gene for the muscle protein titin (*TTN*), shiver at low frequency, fail to maintain body temperatures (T_b) at ambient temperatures (T_a) <34°C, and have reduced body mass and active muscle stiffness *in vivo* compared with wild-type (WT) siblings. Impaired shivering thermogenesis (ST) could be due to the mutated titin protein causing more compliant muscles. We hypothesized that non-shivering thermogenesis (NST) is impaired. To characterize the response to cold exposure, we measured T_b and metabolic rate (MR) of WT and *mdm* mice at four nominal temperatures: 20, 24, 29 and 34°C. Subsequently, we stimulated NST with noradrenaline. Manipulation of T_a revealed an interaction between genotype and MR: *mdm* mice had higher MRs at 29°C and lower MRs at 24°C compared with WT mice. NST capacity was lower in *mdm* mice than in WT mice. Using MR data from a previous study, we compared MR of *mdm* mice with MR of *Perognathus longimembris*, a mouse species of similar body mass. Our results indicated low MR and reduced NST of *mdm* mice. These were more pronounced than differences between *mdm* and WT mice owing to body mass effects on MR and capacity for NST. Correcting MR using Q_{10} showed that *mdm* mice had lower MRs than size-matched *P. longimembris*, indicating that mutated N2A titin causes severe thermoregulatory defects at all levels. Direct effects of the titin mutation lead to lower shivering frequency. Indirect effects likely lead to a lower capacity for NST and increased thermal conductance through decreased body size.

KEY WORDS: Body temperature regulation, Non-shivering thermogenesis, Muscular dystrophy with myositis, Metabolism

INTRODUCTION

Defense of a constant core body temperature (T_b) by generating or dissipating heat is the defining feature of homeothermic endotherms. Thermoregulatory heat production and heat loss allows small animals to maintain thermal constancy even when challenged with temperatures outside of their thermal neutral zone. Large deviations in T_b can have severe consequences, such as reduced enzyme efficiency, altered diffusion capacity and changes in membrane fluidity. These critical cellular functions can result in loss of consciousness, inability to coordinate and execute motor functions, and even death (Morrison and Nakamura, 2011). T_b is maintained during cold exposure by vasoconstriction of peripheral vessels, piloerection, postural changes, shivering thermogenesis (ST) and regulatory non-shivering thermogenesis (NST; Hemingway, 1963). A previous study found that mice with a mutation in the gene for the muscle protein titin (*TTN*) exhibit decreased tremor frequency during ST and could not maintain euthermic T_b when exposed to ambient temperatures (T_a) <34°C (Taylor-Burt et al., 2015). In this study, we investigated the effect of the titin mutation on the other heat-generating mechanism, NST.

NST is a heat-generating mechanism that occurs through the uncoupling of oxidative phosphorylation and ATP production by uncoupling protein-1 (UCP1) in brown adipose tissue (BAT). UCP1 is expressed among many animals, including rodents (Cannon and Nedergaard, 2004; Depocas, 1960; Golozoubova, 2006; Lowell et al., 1993; Meyer et al., 2010; Nedergaard et al., 2001; Nicholls and Locke, 1984). Like basal metabolic rate (BMR), the contribution of NST to summit metabolism (summit oxygen consumption rate, $\dot{V}_{O_2sum}$) as well as $\dot{V}_{O_2sum}$ itself, scales with body mass (Wunder and Gettinger, 1996). Thermogenic capacity, which can be approximated by $\dot{V}_{O_2sum}$, provides an estimate of an animal's ability to thermoregulate and refers to the total capacity for heat production during cold exposure. Thermogenic capacity can be measured when both ST and NST are maximally activated during acute cold exposure. The house mouse (*Mus musculus*), has a small body mass, which leads to relatively high thermal conductance and a greater contribution of NST to $\dot{V}_{O_2sum}$ in order to offset heat loss in comparison with larger animals (Wunder and Gettinger, 1996).

The muscular dystrophy with myositis (*mdm*) mouse has a 779-bp deletion in the N2A region of the titin gene *TTN* (Garvey et al., 2002), and a previous study demonstrated severe thermoregulatory deficiencies (Taylor-Burt et al., 2015). Mice homozygous for the *mdm* mutation exhibit severe and progressive degeneration of skeletal muscles and lower body mass, stiffer gait and reduced lifespan compared with wild-type (WT) littermates (Garvey et al., 2002; Huebsch et al., 2005; Lopez et al., 2008). Muscle in *mdm* mice has higher passive stiffness than WT muscle (Hessel et al., 2017; Lopez et al., 2008; Monroy et al., 2017). Taylor-Burt et al. (2015) demonstrated *in vitro* that *mdm* mice have lower active muscle stiffness as well and a lower tremor frequency during ST. It is expected that if titin did not contribute to active muscle stiffness, then the titin mutation in *mdm* mice would not affect tremor frequency. However, tremor frequencies are dramatically reduced in *mdm* mice (Taylor-Burt et al., 2015). The deficiency in shivering frequency likely leads to the observed hypothermic state of *mdm* mice at temperatures below 34°C. The combination of increased thermal conductance and lower heat generation via ST results in an offset between heat production and heat loss, resulting in a failure to adequately thermoregulate even at T_a values modestly below the T_b set-point. Although no studies have previously investigated NST in *mdm* mice, the hypothermic state of *mdm* mice motivated us to determine whether an impairment in NST is also contributing to the decreased heat production.

Center for Bioengineering Innovation, Northern Arizona University, Flagstaff, AZ 86011, USA.

*Author for correspondence (cam523@nau.edu)

C.A.M., 0000-0002-5690-766X; C.L.B., 0000-0001-6008-7257; K.C.N., 0000-0001-8252-0285

Received 14 January 2019; Accepted 10 April 2019

Journal of Experimental Biology (2019) 222, jeb198564. doi:10.1242/jeb.198564

List of symbols and abbreviations

BAT	brown adipose tissue
BMR	basal metabolic rate
mdm	muscular dystrophy with myositis
MR	metabolic rate
NST	non-shivering thermogenesis
RMR	resting metabolic rate
ST	shivering thermogenesis
Ta	ambient temperature
T_b	body temperature
UCP1	uncoupling protein-1
$\dot{V}_{O_2}$	oxygen consumption rate
$\dot{V}_{O_2sum}$	summit oxygen consumption rate
WT	wild type

We set out to determine whether *mdm* mice have impaired NST and whether this contributes to their observed hypothermia in addition to impaired ST and higher thermal conductance as compared with the WT mouse. We tested two hypotheses: (1) MR of *mdm* mice is greater at higher T_a than WT mice owing to a shifted thermoneutral zone (TNZ) of *mdm* mice; and (2) the inability to defend T_b cannot be explained solely by lower shivering frequencies; therefore, an impairment in the other heat-production mechanism, NST, is present.

MATERIALS AND METHODS

Animal experiments were approved by the Institutional Animal Care and Use Committee of Northern Arizona University, under protocol 05-014-R3, which is accredited by the Association for Assessment and Accreditation of Laboratory Animal Care, International.

Mice

Breeding pairs of B6C3Fe *a-/a-mdm* mice (*Mus musculus* Linnaeus 1758) from the Jackson Laboratory (Bar Harbor, ME, USA) were housed on a 14 h:10 h light:dark cycle at 23–24°C at Northern Arizona University. In this study, all animals were housed in an environmental chamber set to 34°C upon weaning, and experiments were conducted during the dark phase of the light cycle, when mice are active. WT mice were fed LabDiet 5001 Laboratory Rodent Diet and *mdm* mice were fed LabDiet 5LJ5 PicoLab High Energy Mouse Diet (LabDiet, St Louis, MO, USA). *mdm* mice were provided the high-fat-diet chow owing to high mortality rates when fed standard laboratory chow. WT mice were housed singly or with siblings and *mdm* mice were housed with the mother and other *mdm* siblings owing to mortality if separated. Each cage was equipped with bedding and enrichment.

Sample sizes for WT and *mdm* mice at each experimental temperature were as follows: 20°C (n=7 WT, n=5 *mdm*), 24°C (n=6 WT, n=7 *mdm*), 29°C (n=6 WT, n=8 *mdm*) and 34°C (n=7 WT, n=8 *mdm*), unless otherwise noted. Body mass differed significantly between genotypes (Welch's test, P<0.001), with *mdm* mice (7.2±0.21 g; n=9) at approximately one-third of the mass of the WT mice (26.0±1.82 g; n=7).

Surgery

To measure core T_b, recording devices were surgically placed in each mouse's peritoneal cavity at the age of 25–30 days. Different temperature recording devices were used because of the smaller size of the *mdm* mice compared with WT siblings. *mdm* mice were implanted with a Biothermo13 passive integrated transponder (PIT) tag (0.109±0.030 g; Biomark, Boise, ID, USA). The PIT tag measured and recorded T_b at a resolution of ±0.5°C. WT mice were implanted with a PhysioTel TA-F10 telemetry device (1.6 g; Data Sciences International, St Paul, MN, USA), which measured T_b at a resolution of ±0.05°C. The surgical protocol was modified from Richter et al. (2017). Briefly, mice were anesthetized with isoflurane USP (MWI Veterinary Supply, Boise, ID, USA) using a Forane vaporizer (Ohio Medical Corporation, Gurnee, IL, USA). Anesthesia was induced by placing the mouse in a small chamber supplied with a 1–2% isoflurane–oxygen mixture. Upon unconsciousness, the mouse was transferred to a heating pad, where anesthesia was administered using a nosecone that delivered a 1–2% oxygen–isoflurane mixture. Once pedal reflex was absent, the abdominal fur was shaved and the exposed skin was scrubbed with povidone iodine and 70% ethanol. The skin and muscle were incised and bluntly dissected to expose the peritoneal cavity. The device was then placed freely inside the peritoneal cavity and the muscle and skin were closed with 3-0 Maxon absorbable monofilament suture. Buprenorphine, an analgesic agent, was administered subcutaneously (0.10 mg kg^{-1}) for 72 h following surgery. Post-surgery recovery lasted for 7 days at 34°C before further experiments were conducted.

Temperature manipulations

Respirometry was conducted as in Richter et al. (2015) and modified for mice. Briefly, mice were placed in 9 liter metabolic cages during the experiments. Oxygen consumption rate ($\dot{V}_{O_2}$) and carbon dioxide (CO_2) production were measured using an open-flow respirometry system (Promethion, Sable Systems International, Las Vegas, NV, USA). Each cage had its own gas analysis chain for respiratory gases comprising a flow controller, capacitive water vapor partial pressure analyzer, spectrophotometric CO_2 analyzer and fuel cell O_2 analyzer. Water vapor was continuously measured and its dilution effect on O_2 and CO_2 was compensated mathematically. The flow rate was maintained at 2 l min^{-1} and subsampled at 250 ml min^{-1}, resulting in ∼12 complete air exchanges per hour. The gas analyzers were calibrated using 100% N_2 and a span gas with a known concentration of CO_2 mixed with N_2 prior to each set of experiments for an animal. The cages were housed inside an environmental chamber (Percival Scientific, Perry, IA, USA) so that T_a could be controlled. Bedding was removed from each cage prior to metabolic trials. Cages sat on top of either an antennae or telemetry receiver (Biomark; Data Sciences International) to collect T_b data throughout the experiment. T_b was recorded once per minute using either PhysioTel RPC-1 Receivers for the PhysioTel TA-F10 telemetry devices or HPR Plus PIT Tag Reader and Antennae for the BioTherm13 PIT tags (Data Sciences International; Biomark). T_a was recorded once per minute using a datalogger (Onset HOBO Data Logger, Bourne, MA, USA) with a resolution of ±0.14°C.

$\dot{V}_{O_2}$ and CO_2 were recorded once per second using SableScreen v3.3.11 acquisition software, with 60 samples averaged per minute for final analysis (Sable Systems International). $\dot{V}_{O_2}$ (ml min^{-1}) is expressed as ml O_2 g^{-1} body mass h^{-1} for each animal and is referred to hereafter as MR. Raw data were processed using ExpeData v1.8.4 (Sable Systems International). A subset of 10 min of each metabolic trial was selected for analysis based upon the following criteria: (1) recordings occurred after the fasting period; (2) T_a did not exceed the specified temperature range for that experiment (20, 24, 29 and 34°C); and (3) the 10 data points for oxygen consumption (ml O_2 g^{-1} h^{-1}) occurred when animal movement was minimal. Movement was assessed by BXYZ-R beam arrays (Sable Systems International).

Journal of Experimental Biology (2019) 222, jeb198564. doi:10.1242/jeb.198564

All mice underwent four 4-h (*mdm*) or 5-h (WT) experiments where T_a was manipulated once per day for four consecutive days. To minimize the effect of diet-induced thermogenesis, WT mice were fasted for 2 h at the onset of the experiment and *mdm* mice were fasted for only 1 h due to their fragility. All mice were weighed before and after each experiment. When calculating mass-specific MR, mass was assumed to be lost linearly across the experimental period. The experimental temperatures (20, 24, 29 and 34°C) were chosen based on a previous study which found that 34°C was the lower critical limit of the TNZ in *mdm* mice (Taylor-Burt et al., 2015). The T_a=34°C was used to establish resting MR for this study.

Q_{10} effects on MR

Because *mdm* mice fail to maintain euthermic T_b below 34°C (Taylor-Burt et al., 2015), we corrected MR of *mdm* mice assuming a Q_{10} of 2.4 (Hudson and Scott, 1979) using the following equation:

$$\mathrm{MR}_{\mathrm{expected}} = \mathrm{MR}_{\mathrm{observed}} Q_{10}^{\frac{(37 - T_{\mathrm{observed}})}{10}}, \quad (1)$$

where $\mathrm{MR}_{\mathrm{expected}}$ is MR expected if T_b is 37°C, $\mathrm{MR}_{\mathrm{observed}}$ is observed MR and T_{observed} is observed T_b. Once $\mathrm{MR}_{\mathrm{expected}}$ was calculated, it was subtracted from $\mathrm{MR}_{\mathrm{observed}}$ to estimate Q_{10} effects and is referred to hereafter as E–O MR.

Noradrenaline-stimulated thermogenesis

To compare the capacity for NST between genotypes, we first fasted mice either for 1 or 2 h (*mdm* and WT, respectively; Speakman, 2013) at 34°C, measured MR (as above) and then briefly removed them from the metabolic cages to subcutaneously administer 1.2 mg kg^{-1} of noradrenaline (Wunder and Gettinger, 1996). Mice were then placed back into the metabolic cages and measured for MR and T_b over the next 2–3 h. The duration of the metabolic curve, referred to as total effect time, as well as time to peak MR and peak MR were measured to test for differences in noradrenaline response between genotypes. In addition, peak T_b and average T_b were compared between genotypes after noradrenaline injection to test whether T_b followed the same trend as MR. Peak T_b was defined as the highest 60 s average, and average T_b was the average T_b during the test.

Thermogenic capacity

Thermogenic capacity can be approximated by $\dot{V}_{O_2\mathrm{sum}}$ (Wunder and Gettinger, 1996) as:

$$\dot{V}_{O_2\mathrm{sum}} = \mathrm{BMR} + \mathrm{ST} + \mathrm{NST}, \quad (2)$$

where $\dot{V}_{O_2\mathrm{sum}}$ is summit metabolism, BMR is basal MR, ST is shivering thermogenesis and NST is non-shivering thermogenesis. $\dot{V}_{O_2\mathrm{sum}}$ is referred to hereafter as thermogenic capacity. Relative contributions of ST, NST and BMR to thermogenic capacity were calculated by rearranging the above equation. MR at 34°C was used for calculations of BMR. To calculate NST, BMR was subtracted from peak MR during noradrenaline-stimulated thermogenesis (n=6 WT, n=6 *mdm*) to parse out MR due solely to NST. Because the mice may not have been post-absorptive during either experiment, NST was likely underestimated and metabolic measurements may have been overestimated. Therefore, we will refer to BMR hereafter as resting metabolic rate (RMR). Taylor-Burt et al. (2015) previously reported thermogenic capacity; therefore, ST was calculated by subtracting peak MR during noradrenaline-stimulated thermogenesis (RMR+NST) from thermogenic capacity.

Statistical analysis

Statistical analysis was performed using JMP v12 (SAS Institute, Inc., Cary, NC, USA). Values are reported as means±s.e.m. and an alpha level of 0.05 was used for all tests. For statistical analysis, body mass was normally distributed but variance of residuals was unequal between groups, so a Welch's test, where the means are weighted by the reciprocal of the group mean variances, was used to identify significant differences. Throughout the study, the *mdm* group at 20°C had a large within-group variance with an outlier, leading to unequal variances when compared with WT mice. Therefore, we used two statistical methods to analyze $\dot{V}_{O_2}$ with and without the outlier. For our primary and more conservative method, data were ranked using temperature as a blocking variable (20, 24, 29 and 34°C). A mixed-model ANOVA with subject nested within genotype and fixed effects of temperature and genotype was conducted for T_b, MR and Q_{10} effects data. Steel–Dwass multiple comparisons were used to identify significant differences between genotypes at all temperatures. In our secondary method with the outlier removed, residuals of the $\dot{V}_{O_2}$ data were normally distributed with equal variance; therefore, data were analyzed using two-way ANOVA with subject nested within genotype and fixed effects of temperature and genotype. Tukey's HSD test was conducted *post hoc*. Removing the outlier for the E–O MR data did not change statistical significance, so this was not reported. For the noradrenaline-stimulated thermogenesis data, Welch's test for unequal variances was used to identify significant differences in peak T_b, average T_b and time to peak. *t*-tests were used for peak MR, total effect time and NST capacity. To identify significant differences in absolute contributions to thermogenic capacity, *t*-tests were used to compare ST and NST between genotypes.

For calculations of noradrenaline-stimulated thermogenesis, subsequent rise in MR after noradrenaline injection yielded a metabolic curve from which thermogenic capacity due to NST was calculated by taking the integral of the increase in MR after noradrenaline injection, computed numerically using the trapezoidal rule. The average of 10 consecutive minutes of MR measures that met the criteria (as above) before the animal was removed from the cage was considered their baseline MR. This was subtracted from the calculation to account for animals that had higher or lower $\dot{V}_{O_2}$ before injection. The area calculation began with the onset of injection and ended when $\dot{V}_{O_2}$ reached previously calculated baseline values.

RESULTS

Body temperature

mdm mice exhibited hypothermic characteristics, as shown by their lower T_b values in comparison with WT mice at lower T_a. There was a significant effect of genotype and T_a on T_b (P<0.001) but no interaction between T_a and genotype. We found a significant effect of subject (P<0.05). *Post hoc* tests revealed significant differences between genotypes at all temperatures (P<0.05; Fig. 1). At 20, 24, 29 and 34°C, we observed the following differences in T_b between WT and *mdm* mice, respectively: 8.8, 4.2, 1.9 and 1.4°C.

Metabolic rate

At 24°C, thermoregulatory mechanisms in *mdm* mice are insufficient to maintain constant and euthermic T_b, resulting in significantly lower MR (Fig. 2) and T_b (Fig. 1) as compared with WT mice. In addition, *mdm* mice activate ST and NST more than WT mice at 29°C, as demonstrated by their higher MR. Despite their higher MR, their T_b remained lower than that of WT mice.

There was a significant interaction between genotype and temperature on MR (P<0.05). The MRs of WT and *mdm* mice did

Journal of Experimental Biology (2019) 222, jeb198564. doi:10.1242/jeb.198564

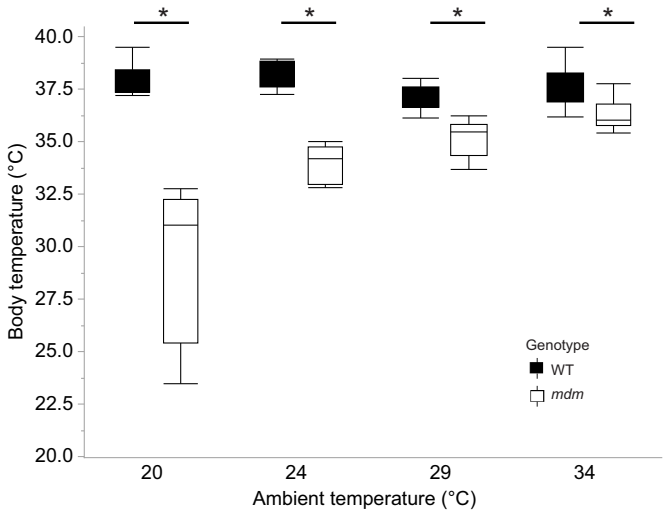

Fig. 1. The relationship between body temperature (T_b) and ambient temperature (T_a) in wild-type (WT) and *mdm* mice. Temperatures used were within a range of T_a beginning at the thermoneutral zone of *mdm* mice (Taylor-Burt et al., 2015) and ending at lower T_a in order to observe how well T_b could be defended (*P<0.05). *mdm*, muscular dystrophy with myositis.

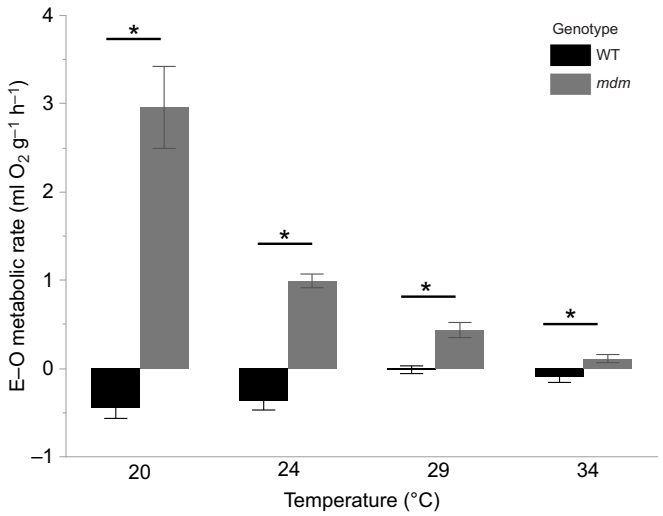

Fig. 3. The relationship between expected–observed (E–O) MR and T_a. The Q_{10} equation was rearranged to find $MR_{expected}$ if mice had a T_b of 37°C and a Q_{10} of 2.4 (Hudson and Scott, 1979), and $MR_{expected}$ was compared with $MR_{observed}$ to investigate T_b effects on MR between genotypes (*P<0.05). $MR_{expected}$, expected metabolic rate; $MR_{observed}$, observed metabolic rate.

not significantly differ at 34°C (P>0.05). At 29°C, the MR of *mdm* mice (2.4±0.12 ml O_2 g^{-1} h^{-1}) was significantly higher than that of WT mice (1.9±0.09 ml O_2 g^{-1} h^{-1}; P<0.05). At 24°C, the MR of WT mice (3.9±0.19 ml O_2 g^{-1} h^{-1}) was significantly higher than that of *mdm* mice (3.1±0.34 ml O_2 g^{-1} h^{-1}). WT mice (4.8±0.29 ml O_2 g^{-1} h^{-1}) did not have significantly different MRs from *mdm* mice (3.5±1.51 ml O_2 g^{-1} h^{-1}) at 20°C (P=0.1939); this was likely due to the large variability in *mdm* MR at 20°C compared with WT mice (Fig. 2). When the *mdm* outlier at 20°C was removed, MRs of WT mice at 20°C were significantly higher than those of *mdm* mice. Additionally, the *mdm* mean MR dropped to 2.9±0.89 ml O_2 g^{-1} h^{-1} as opposed to 3.5±1.51 ml O_2 g^{-1} h^{-1}.

Q_{10} effects on MR

In general, *mdm* mice had $MR_{observed}$ values far lower than $MR_{expected}$ values, with the largest differences in E–O MR at the lower temperatures (Fig. 3). WT mice tended to remain close to $MR_{expected}$, except at lower temperatures, where $MR_{observed}$ was higher than predicted. The higher E–O MR values for WT mice at lower temperatures are likely a result of certain subjects having higher activity, and thus higher MR at lower temperatures (observational).

A significant effect of genotype was found on E–O MR: *mdm* mice had significantly higher E–O MR compared with WT mice at all temperatures (P<0.001). The largest differences in E–O MR were seen at the two lowest temperatures. At 24°C, *mdm* mice (1.0±0.08 ml O_2 g^{-1} h^{-1}) had significantly higher E–O MR than WT mice (−0.4±0.10 ml O_2 g^{-1} h^{-1}; P<0.05), which had higher observed values than predicted, making their E–O MR negative. At the lowest temperature of 20°C, *mdm* mice (3.0±0.46 ml O_2 g^{-1} h^{-1}) failed to attain their expected MR. WT mice, in contrast, had higher observed than expected values (0.4±0.32 ml O_2 g^{-1} h^{-1}; P<0.05).

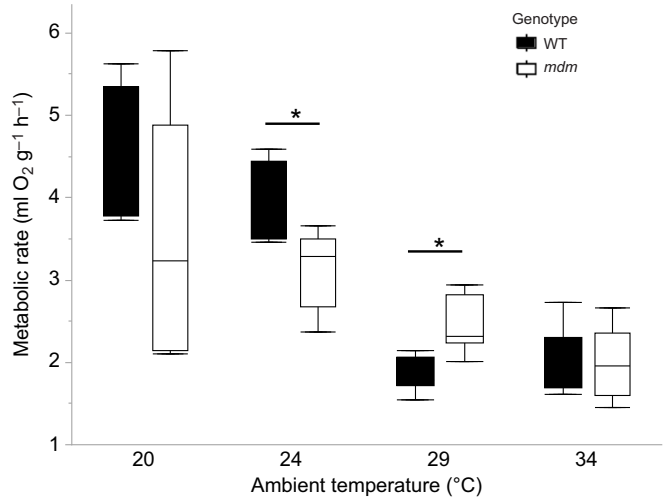

Fig. 2. The relationship between metabolic rate (MR) and T_a. Temperatures used were within a range starting at the thermoneutral zone for *mdm* mice, where MR was expected to be at resting levels, to lower T_a at which MR was expected to increase (*P<0.05).

Noradrenaline-stimulated thermogenesis

Both WT and *mdm* mice exhibited similar metabolic profiles following noradrenaline injection, but WT mice had a significantly higher capacity for NST, found using area under the curve (143.9±20.01 ml O_2 g^{-1} h^{-1}), than *mdm* mice (62.3±22.78 ml O_2 g^{-1} h^{-1}; P<0.05; Fig. 4). There were no significant differences between genotypes in either latency to reach peak MR (P=0.60) or the total effect time (P=0.08; Fig. 4). WT mice took 17.3±2.20 min to reach peak MR and *mdm* mice took 22.8±9.65 min. Total effect time for WT and *mdm* mice was 66.3±4.92 min and 48.3±10.44 min, respectively. Interestingly, genotypes did not differ in peak MR reached after injection (P=0.21), with WT mice reaching 7.2 ml O_2 g^{-1} h^{-1} and *mdm* mice reaching 6.4 ml O_2 g^{-1} h^{-1}. However, WT mice (39.7±0.08°C) reached a higher peak T_b (P<0.05) than *mdm* mice (38.5±0.35°C) during the trial. In addition, WT mice had a significantly higher average T_b (38.7±0.24°C) than *mdm* mice (37.3±0.33°C; P<0.05).

DISCUSSION

In this study, we examined the capacity for NST in *mdm* mice to investigate whether this component of heat production is impaired.

Journal of Experimental Biology (2019) 222, jeb198564. doi:10.1242/jeb.198564

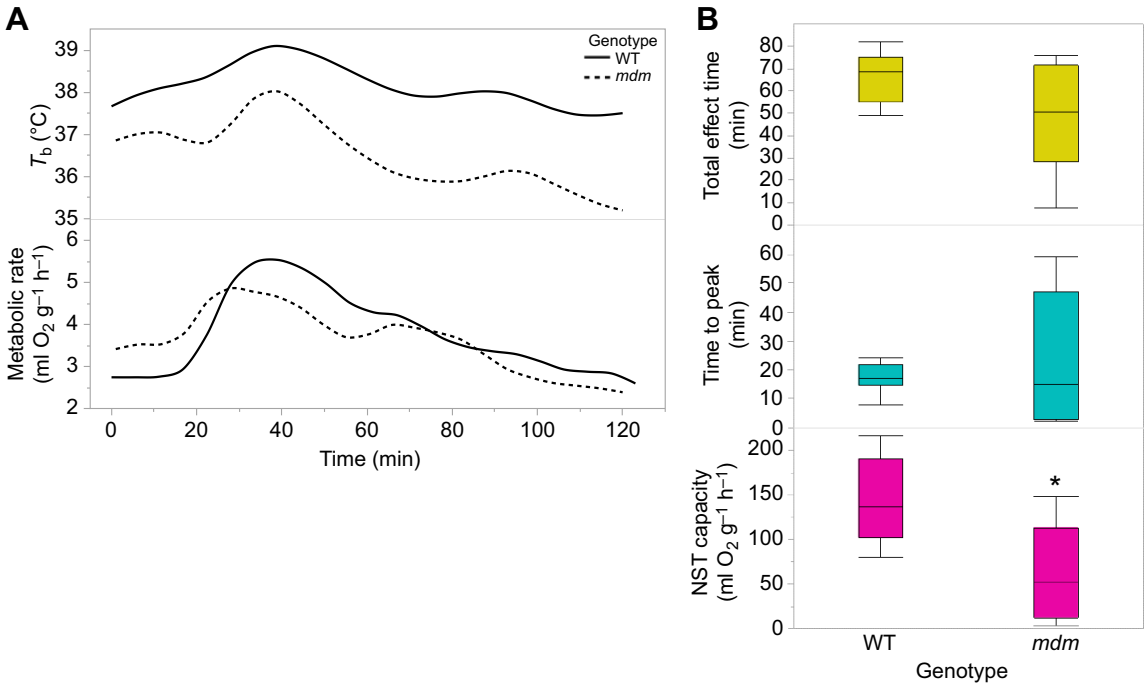

Fig. 4. Responses to noradrenaline in WT and *mdm* mice. (A) T_b and MR responses to noradrenaline in WT and *mdm* mice. WT mice had significantly higher peak T_b and average T_b compared with *mdm* mice (n=6 WT, n=6 *mdm*; Welch's test, P<0.05). Genotypes did not differ in peak MR (t-test, P=0.11). (B) Total effect time, time to reach peak MR and area under the curve between genotypes after noradrenaline injection. *mdm* mice had a smaller area underneath the metabolic curve, and thus a lower capacity for NST after noradrenaline injection (1.2 mg^{-1} kg^{-1}) compared with WT mice (n=6 WT, n=6 *mdm*; *P<0.05). The amount of time it took to reach peak MR was not significant between groups (P=0.60), nor was the total effect time of noradrenaline on MR (P=0.08). NST, non-shivering thermogenesis.

Our results demonstrate that a deletion in the titin gene *TTN* not only results in a deficiency in ST, but it impacts NST as well, likely contributing to lower T_b, MR and thermogenic capacity. Previously, it was shown that the capacity for ST of *mdm* mice is compromised (Taylor-Burt et al., 2015). We confirmed the inability of *mdm* mice to maintain homeothermy by measuring their T_b and MR across a range of T_a values. Compared with WT mice, *mdm* mice had lower T_b values at all T_a values and lower MRs at 24°C. Because *mdm* mice could not defend core T_b, we observed significant Q_{10} effects on MR. E–O MR was significantly higher for *mdm* mice. Further, we found that the capacity for NST was significantly lower in *mdm* mice compared with WT mice, indicating that this component of heat generation is also impaired. The relative contributions of basal MR, ST or NST to $\dot{V}_{O_2sum}$ did not differ between WT and *mdm* mice.

Body temperature

mdm mice had significantly lower T_b values than WT mice, even at 34°C (Fig. 1). These findings suggest that in order for *mdm* mice to have a euthermic T_b set-point similar to that of WT mice, T_a needs to be even higher than 34–35°C, as previously reported by Taylor-Burt et al. (2015) for *mdm* mice to maintain euthermy.

We do not think that *mdm* mice are entering torpor at the temperatures they were tested. A reduction in T_b set-point due to torpor is unlikely owing to the pattern of MR and T_b observed. Torpor is characterized by a 'decided' reduction in T_b set-point that leads to a precipitous decline in MR and T_b (Geiser et al., 2014). During hypothermia, T_b set-point is at euthermic levels, but the animal cannot support the metabolic heat production needed to maintain euthermia; therefore, both T_b and MR decrease slowly as thermoregulatory mechanisms fail to meet demand and then decline rapidly once the body cools further. *mdm* mice exhibited increases in MR upon cold exposure followed by a gradual reduction, which was likely hypothermia. This indicates that thermoregulatory mechanisms of *mdm* mice are insufficient to maintain T_b. Hudson and Scott (1979) measured T_b and MR in *M. musculus* and found that torpid mice with T_b of 32°C had a metabolism 50% of what was observed at euthermic T_b levels. The mice in our study had similar T_b values of ∼29.3°C at 20°C but had higher MRs of ∼3.5 and ∼2.0 ml O_2 g^{-1} h^{-1} at 20 and 34°C, respectively, suggesting that *mdm* mice lack sufficient thermoregulatory capacity at T_a values <34°C and do not adopt the behavioral strategy of hypometabolism through torpor.

Studies have shown thermoregulatory deficiencies specific to NST in UCP1-null mice, mice with induced obesity and Type II diabetes due to leptin alterations (*ob/ob* and *db/db*), and mice with inherited defects of fatty acid oxidation. UCP1-null mice were able to acclimate and tolerate 18°C with a well-defended T_b that was not significantly different from that of WT mice (Golozoubova, 2006). Similarly, administration of leptin to ground squirrels failed to alter their thermogenic capacity (Boyer et al., 1997). However, adaptive NST was significantly altered in UCP1-null mice (details below). Mice with induced rapid early-onset obesity (*ob/ob*) and diabetes (*db/db*) have markedly reduced capacity for NST (Yen, et al., 1974). T_b of *ob/ob* and *db/db* mice was 30±1.4°C and 26.8±8°C, respectively, after 90 min of exposure to 4°C. This is comparable to *mdm* mice at 20°C, with T_b values of 29.3±1.2°C. In addition, mice homozygous for the inactivated allele BALB/cByJ, which encodes the short-chain acyl CoA dehydrogenase, have abnormal NST (Guerra et al., 1998). In BALB/cByJ mice, T_b decreased by 10°C in less than 4 h at 4°C, which is similar to *mdm* mice at 20°C.

The impact of ST on maintenance of T_b can be assessed by blocking muscular activity via curare-like drugs, which competitively block the binding of acetylcholine to the motor endplates of striated muscles (Bowman, 2006; Kashimura et al.,

Journal of Experimental Biology (2019) 222, jeb198564. doi:10.1242/jeb.198564

1992). In a study that reduced shivering by 50% via curare, WT mice were still able to maintain a T_b of 35.4±0.4°C at 4°C (Bal et al., 2012), likely because of their ability to compensate via NST. It is difficult to compare thermoregulatory deficits of *mdm* mice with those of genetically altered mice in other studies owing to 4°C being the standard cold temperature versus 20°C, which was used in our study as this is the low temperature limit of *mdm* mice. Nonetheless, the *mdm* mice in our study expressed more severe thermoregulatory defects than mice with deficits in either ST or NST discussed above. This is likely due to the combined defects of both ST and NST in *mdm* mice.

Metabolic rate

mdm and WT mice maintained similar RMRs at a T_a of 34°C (Fig. 2). These values are slightly higher but comparable to resting MRs reported for *M. musculus* that were fasted between 5 and 30 h (Hudson and Scott, 1979). The mice in our study were fasted for only 2 h (WT) or 1 h (*mdm*), which could account for the slightly higher MRs we found.

mdm mice reach thermoregulatory failure at T_a values below 29°C and are more cold-stressed than WT mice at this T_a. This is demonstrated by significantly higher MRs of *mdm* mice compared with WT mice (Fig. 2). WT mice had comparable MRs at 34°C and 29°C likely because these T_a values are near or within their TNZ (31–35°C; Hudson and Scott, 1979). Interestingly, although *mdm* mice have higher MRs than WT mice at 29°C, they maintained a significantly lower T_b. These results indicate that at this T_a, *mdm* mice work harder than WT mice to thermoregulate, yet they still cannot maintain or attain euthermic T_b and are thus hypothermic. The failure to maintain a higher T_b despite higher MRs is likely due to the combination of increased thermal conductance of the much smaller *mdm* mice and their compromised thermoregulatory capacity.

At 24°C, there was a large difference in MR between *mdm* and WT mice, with WT mice having significantly higher MRs (Fig. 2). There were no significant differences in MRs between WT and *mdm* mice at 20°C, which was interesting considering T_b differences were even more different between genotypes. This is likely due to the effect of a single outlier in the *mdm* group that greatly increased the standard error of this group as compared with the WT group. When we analyzed the data with the outlier removed, WT mice had significantly higher MRs than *mdm* mice.

As previously stated, MR scales with body size and it is necessary to account for the much smaller size (7 g) of *mdm* mice and its impact on MR. A similarly sized mouse, *Perognathus longimembris* (little pocket mouse), is highly abundant and one of the smallest rodents in North America (Bartholomew and Cade, 1957). Previous groups have studied this species because of its ability to maintain homeothermy despite its small size. A previous study investigating MR of the little pocket mouse reported regressions across T_a values (Chew et al., 1967) to investigate allometric scaling of MR with T_a (Kleiber, 1932). This allowed us to compare MR of the little pocket mouse with MR of *mdm* mice (using Q_{10}-corrected MR) at our desired T_a. For each of the temperature ranges (20, 24, 29 and 34°C), differences in $MR_{expected}$ between the little pocket mouse and *mdm* mice were as follows: 0.54, 1.69, 1.65 and 0.85 ml O_2 g^{-1} h^{-1}. Surprisingly, $MR_{expected}$ of *mdm* mice was less than predicted MRs for the size-matched little pocket mouse at all of the test temperatures.

Our data indicate that even if *mdm* mice could obtain euthermic T_b, they would still have a deficit in MR. E–O MR of WT and *mdm* mice differed significantly at all T_a values. In general, WT mice had $MR_{expected}$ close to $MR_{observed}$, leading us to conclude that their Q_{10} approximated 2.4, which is typical of euthermic *M. musculus* (Hudson and Scott, 1979). The T_b data also confirm that WT mice were euthermic for all trials (Fig. 1). *mdm* mice, in contrast, had much higher $MR_{expected}$ than $MR_{observed}$, leading to high E–O MR.

Non-shivering thermogenesis

Maximal $\dot{V}_{O_2}$ following noradrenaline injection correlates well with body mass and is affected by acclimation temperature, with cold-acclimated animals having higher $\dot{V}_{O_2}$ responses. Allometric relationships for maximal metabolic response to noradrenaline in small mammals have been described by Wunder and Gettinger (1996) and include a BMR component that can be used for animals acclimated to 23°C. Using this equation, the $\dot{V}_{O_2}$ response of WT and *mdm* mice to noradrenaline was predicted to be 6 and 11 ml O_2 g^{-1} h^{-1}, respectively. Observed maximal $\dot{V}_{O_2}$ responses to noradrenaline values for WT and *mdm* mice were 7.2 and 6.4 ml O_2 g^{-1} h^{-1}, which did not significantly differ. WT mice did not differ from the Wunder model output and *mdm* mice failed to increase MR after noradrenaline injection accordingly. These conclusions are also reflected in the NST contributions to thermogenic capacity (Fig. 5). These comparisons provide further evidence that *mdm* mice have a lower $\dot{V}_{O_2}$ response to noradrenaline than WT mice.

Although *mdm* mice have a lower capacity for NST, the latency from noradrenaline injection to peak MR, total effect time of noradrenaline, and peak MR were similar to WT mice (Fig. 4). Peak T_b and average T_b of WT mice were significantly higher after noradrenaline injection than in *mdm* mice (Fig. 4). These results are consistent with the finding that *mdm* mice have a reduced capacity for NST. Similarly, *mdm* mice were unable to maintain euthermic T_b. This could have been due to their increased thermal conductance or to a depletion of metabolic fuels needed for NST, primarily free fatty acids and glucose (Townsend and Tseng, 2014).

Based on the severe phenotype of the *mdm* mice compared with UCP1-null mice, the null hypothesis is that the lower capacity of NST in *mdm* mice is due to the absence of UCP1. In WT and UCP1-null mice that were warm-acclimated to 30°C, noradrenaline evoked large increases in MR for WT mice and small increases for

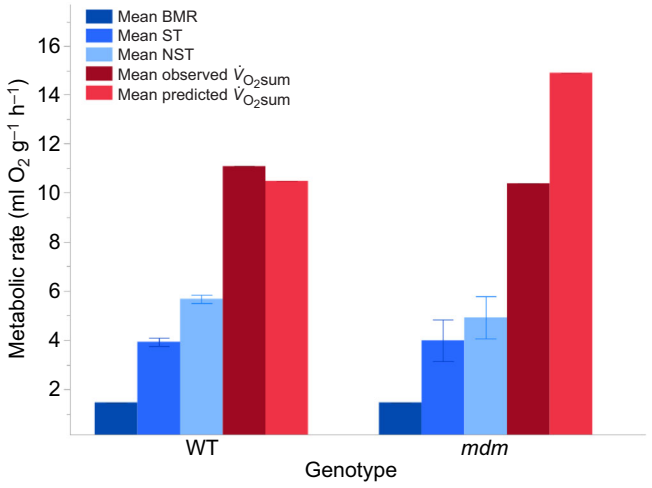

Fig. 5. Contributions of basal metabolic rate (BMR), shivering thermogenesis (ST) and NST to observed thermogenic capacity ($\dot{V}_{O_2sum}$) and predicted $\dot{V}_{O_2sum}$ in WT and *mdm* mice. WT and *mdm* mice did not differ significantly in the contributions of BMR (P>0.05), ST (P=0.53) and NST (P=0.21) to thermogenic capacity (n=6 WT, n=6 *mdm*; t-tests). Observed thermogenic capacity of *mdm* mice from Taylor-Burt et al.'s (2015) study fell short of predicted thermogenic capacity based on body size.

UCP1-null mice (Golozoubova, 2006). The small increase seen in UCP1-null mice was attributed to either UCP1-independent adrenergic thermogenesis or a general activation of adrenergic receptors. The mice in our study did not have a significantly different peak $\dot{V}_{O_2}$ response to noradrenaline compared with WT mice (Fig. 4); therefore, a solely adrenergic effect causing MR increase in *mdm* is not likely. In this study, we did not quantify expression of UCP1 or excise putative BAT from mice in the study; however, an interesting line of thought is the possibility for decreased UCP1 expression or decreased sensitivity in BAT to noradrenaline in *mdm* mice.

Although only MR and T_b were measured, *mdm* mice appear to be compromised in heat production at the BAT level. It is unlikely they are affected at the sympathetic outflow level based on the results from noradrenaline injection. The NST response was inferred from indirect calorimetry by mimicking a maximal sympathetic response through administration of noradrenaline, which is known to stimulate UCP1 activity in BAT. Because noradrenaline injection resulted in a lower than expected metabolic response and animals could not maintain euthermic T_b, we hypothesize that *mdm* mice are impacted at the level of BAT.

Titin has been implicated as a regulator in mitochondrial respiration as well as bioenergetics. The *sallimus* (*sls*) gene in *Drosophila*, whose product is homologous to the NH2-terminal half of titin in vertebrates, has been identified as a transcription regulator of mitochondrial respiration (Jumbo-Lucioni et al., 2012). Jumbo-Lucioni et al. (2012) observed the natural variation between state 3 and state 4 mitochondrial respiration and found a direct effect of *sls* on mitochondrial function. Homozygous sls^{d00134} flies, which have a missing allele from the *sls* gene, had 17% lower mitochondrial state 3 and 18% higher state 4 rates than controls. These results reveal that *sls* is a novel gene hub for regulation of mitochondrial respiration and that specific alleles of this gene can control naturally occurring variation in mitochondrial function. In addition, truncating titin variants (TTNtv) that cause genetic dilated cardiomyopathy (DCM) have been shown to alter mitochondrial bioenergetics (Verdonschot et al., 2018). In patients with TTNtv, increased expression of genes across all electron transport chain complexes as well as ATP synthase was found. These findings suggest a compensatory response of increased oxidative phosphorylation components in order to counteract limited contractile ability of cardiac tissue as an indirect effect of a titin mutation.

Defects in oxidative phosphorylation can affect BAT thermogenic activity (Kajimura and Saito, 2014). During BAT-mediated thermogenesis, UCP1 uncouples heat production from ATP synthase; therefore, it is likely that defects in oxidative phosphorylation could affect this output. As mentioned above, titin can modulate mitochondrial bioenergetics and transcription of oxidative phosphorylation components, and therefore could be a potential explanation for the reduced NST capacity of *mdm* mice. Taylor-Burt et al. (2015) demonstrated a direct effect of titin stiffness on the rate of ST, and our results indicate that an NST deficiency could reflect a regulatory effect of titin on metabolic processes. Whether these effects are due to titin signaling or other pathways is a question that could be explored in future work.

Thermogenic capacity and its components

Thermogenic capacity is significantly reduced in *mdm* mice compared with expected values for their body size (Fig. 5) (Taylor-Burt et al., 2015). Many small mammals, including deer mice, increase their thermogenic capacity solely by increasing NST after cold acclimation (Van Sant and Hammond, 2008). Although NST is regarded as the most plastic component of $\dot{V}_{O_2sum}$, animals can also increase their capacity for ST after cold acclimation (Nespolo, et al., 1999). This leads to the hypothesis that animals with deficient ST would increase NST capacity to compensate. It is interesting that *mdm* mice have a reduced thermogenic capacity for both ST and NST.

Our results show significant differences in MR as well as the capacity for NST even after accounting for body mass differences (WT mice are approximately four times larger than *mdm* mice). Because of the allometric relationship between body mass, MR and capacity for NST, our comparisons allowed us to conclude that the severe defects in thermoregulation are not just due to body size. Comparisons between *mdm* mice and the little pocket mouse demonstrate that *mdm* mice do not exhibit similar MRs to size-matched animals, as shown by their smaller MRs, even at thermoneutrality (Chew et al., 1967). Additionally, as animals become smaller, the contribution of NST to thermogenic capacity increases to offset the balance in increased thermal conductance due to increased surface area (Wunder and Gettinger, 1996). $\dot{V}_{O_2}$ responses to NE in *mdm* mice were less than half the predicted value (11 ml O_2 g^{-1} h^{-1}; Wunder and Gettinger, 1996). Our findings demonstrate that *mdm* mice do not activate more heat-generating mechanisms like other small animals to offset the increased heat loss owing to small body size, and that their thermoregulatory defects are either due to direct or indirect effects of the N2A deletion in titin.

Conclusions

A previous study showed an unexpected link between a small titin mutation, ST and thermoregulation (Taylor-Burt et al., 2015). The present study expands on the previous study through continuous monitoring of T_b and investigation of NST and MR. A link between titin mutations and metabolic deficits might have implications for understanding inherited diseases due to titin mutations, which are increasingly found in humans. We conclude that a deletion in the N2A titin gene *TTN* reduces not only the rate of ST in *mdm* mice (Taylor-Burt et al., 2015), but also NST. Collectively, *mdm* mice exhibit a significantly compromised thermogenic capacity. When comparisons are made to account for the small body size of *mdm* mice, these deficiencies are exacerbated. It is not clear how titin modulates both NST and body size, but it could be through an indirect role in regulating oxidative phosphorylation or other pathways. Future studies should investigate these possible links.

Acknowledgements

We thank Anthony Hessel, Johhn Lighton, Uzma Tahir, Tinna Traustadóttir and our reviewers for their helpful comments on this manuscript. We would also like to give a special thanks to Danielle Dillon, Destiny Simpson and the team at Sable Systems International for their technical help with this project.

Competing interests

The authors declare no competing or financial interests.

Author contributions

Conceptualization: C.A.M., C.L.B., K.C.N.; Methodology: C.A.M., C.L.B., K.C.N.; Validation: C.A.M.; Formal analysis: C.A.M., K.C.N.; Investigation: C.A.M.; Resources: C.A.M., C.L.B., K.C.N.; Data curation: C.A.M., S.F.; Writing - original draft: C.A.M.; Writing - review & editing: C.A.M., S.F., C.L.B., K.C.N.; Visualization: C.A.M., C.L.B., K.C.N.; Supervision: C.L.B., K.C.N.; Project administration: C.L.B., K.C.N.; Funding acquisition: C.L.B., K.C.N.

Funding

Our funding sources include the National Science Foundation (IOS-0742483, IOS-1025806 and IOS-1456868), the W. M. Keck Foundation, and the Technology Research Initiative Fund of Northern Arizona University.

References

Bal, N. C., Maurya, S. K., Sopariwala, D. H., Sahoo, S. K., Gupta, S. C., Shaikh, S. A., Pant, M., Rowland, L. A., Bombardier, E., Goonasekera, S. A. et al. (2012). Sarcolipin is a newly identified regulator of muscle-based thermogenesis in mammals. *Nat. Med.* **18**, 1575-1579. doi:10.1038/nm.2897

Bartholomew, G. A. Cade, T. J. (1957). Temperature regulation, hibernation, and aestivation in the little pocket mouse. *J. Mammal.* **38**, 60-72. doi:10.2307/1376476

Bowman, W. C. (2006). Neuromuscular block. *Br. J. Pharmacol.* **147**, 277-286. doi:10.1038/sj.bjp.0706404

Boyer, B. B., Ormseth, O. A., Buck, L., Nicolson, M., Pelleymounter, M. A. and Barnes, B. M. (1997). Leptin prevents posthibernation weight gain but does not reduce energy expenditure in arctic ground squirrels. *Comp. Biochem. Physiol.* **118**, 405-412. doi:10.1016/S0742-8413(97)00172-2

Cannon, B. and Nedergaard, J. (2004). Brown adipose tissue: function and physiological significance. *Physiol. Rev.* **84**, 277-359. doi:10.1152/physrev.00015.2003

Chew, R. M., Lindberg, R. G. and Hayden, P. (1967). Temperature regulation in the little pocket mouse, *Perognathus longimembris*. *Comp. Biochem. Physiol.* **21**, 487-505. doi:10.1016/0010-406X(67)90447-1

Depocas, F. (1960). The calorigenic response of cold-acclimated white rats to infused noradrenaline. *Biochem. Cell Biol.* **38**, 107-114. doi:10.1139/o60-012

Garvey, S. M., Rajan, C., Lerner, A. P., Frankel, W. N. and Cox, G. A. (2002). The muscular dystrophy with myositis (mdm) mouse mutation disrupts a skeletal muscle-specific domain of titin. *Genomics 79, 146-149*. doi:10.1006/geno.2002.6685

Geiser, F., Currie, S. E., O'Shea, K. A. and Hiebert, S. M. (2014). Torpor and hypothermia: reversed hysteresis of metabolic rate and body temperature. *AJP Regul. Integr. Comp. Physiol.* **307**, R1324-R1329. doi:10.1152/ajpregu.00214.2014

Golozoubova, V. (2006). UCP1 is essential for adaptive adrenergic nonshivering thermogenesis. *AJP Endocrinol Metabolism* **291**, E350-E357.doi:10.1152/ajpendo.00387.2005

Guerra, C., Koza, R. A., Walsh, K., Kurtz, D. M., Wood, P. A. and Kozak, L. P. (1998). Abnormal nonshivering thermogenesis in mice with inherited defects of fatty acid oxidation. *J. Clin. Investig.* **102**, 1724-1731. doi:10.1172/JCI4532

Hemingway, A. (1963). Shivering. *Physiol. Rev. 43, 397-422*. doi:10.1152/physrev.1963.43.3.397

Hessel, A. L., Lindstedt, S. L. and Nishikawa, K. C. (2017). Physiological mechanisms of eccentric contraction and its applications: a role for the giant titin protein. *Front. Physiol.* **8, 70**. doi:10.3389/fphys.2017.00070

Hudson, J. W. and Scott, I. M. (1979). Daily torpor in the laboratory mouse, *Mus musculus* var. albino. *Physiol. Zool.* **52**, 205-218. doi:10.1086/physzool.52.2.30152564

Huebsch, K. A., Kudryashova, E., Wooley, C. M., Sher, R. B., Seburn, K. L., Spencer, M. J. and Cox, G. A. (2005). Mdm muscular dystrophy: interactions with calpain 3 and a novel functional role for titin's N2A domain. *Hum. Mol. Genet.* **14**, 2801-2811. doi:10.1093/hmg/ddi313

Jumbo-Lucioni, P., Bu, S., Harbison, S. T., Slaughter, J. C., Mackay, T. F. C., Moellering, D. R. and De Luca, M. (2012). Nuclear genomic control of naturally occurring variation in mitochondrial function in *Drosophila melanogaster*. *BMC Genomics* **13**. doi:10.1186/1471-2164-13-659

Kajimura, S. and Saito, M. (2014). A new era in brown adipose tissue biology: molecular control of brown fat development and energy homeostasis. *Annu. Rev. Physiol.* **76**, 225-249. doi:10.1146/annurev-physiol-021113-170252

Kashimura, O., Sakai, A., Yanagidaira, Y. and Ueda, G. (1992). Thermogenesis induced by inhibition of shivering during cold exposure in exercise-trained rats. *Aviat. Space Environ. Med.* **63**, 1082-1086.

Kleiber, M. (1932). Body size and metabolism. *Calif. Agric. Exp. Stn.* **6**, 315-353. doi:10.3733/hilg.v06n11p315

Lopez, M. A., Pardo, P. S., Cox, G. A. and Boriek, A. M. (2008). Early mechanical dysfunction of the diaphragm in the muscular dystrophy with myositis (Ttnmdm) model. *AJP Cell Physiol.* **295**, C1092-C1102. doi:10.1152/ajpcell.16.2008

Lowell, B., S-Susulic, V., Hamann, A., Lawitts, J., Himms-Hagen, J., Boyer, B., Kozak, L. P. and Flier, J. (1993). Development of obesity in transgenic mice after genetic ablation of brown adipose tissue. *Nature* **366**, 740-742. doi:10.1038/366740a0

Meyer, C. W., Willershäuser, M., Jastroch, M., Rourke, B. C., Fromme, T., Oelkrug, R., Heldmaier, G. and Klingenspor, M. (2010). Adaptive thermogenesis and thermal conductance in wild-type and UCP1-KO mice. *Am. J. Physiol. Regul. Integr. Comp. Physiol.* **299**, R1396-R1406. doi:10.1152/ajpregu.00021.2009

Monroy, J. A., Powers, K. L., Pace, C. M., Uyeno, T. and Nishikawa, K. C. (2017). Effects of activation on the elastic properties of intact soleus muscles with a deletion in titin. *J. Exp. Biol.* **220**, 828-836. doi:10.1242/jeb.139717

Morrison, S. F. and Nakamura, K. (2011). Central neural pathways for thermoregulation. *Front. Biosci.* **16**, 74-104. doi:10.2741/3677

Nedergaard, J., Golozoubova, V., Matthias, A., Asadi, A., Jacobsson, A. and Cannon, B. (2001). UCP1: The only protein able to mediate adaptive non-shivering thermogenesis and metabolic inefficiency. *Biochim. Biophys. Acta* **1504**, 82-106. doi:10.1016/S0005-2728(00)00247-4

Nespolo, R. F., Opazo, J. C., Rosenmann, M. and Bozinovic, F. (1999). Thermal acclimation, maximum metabolic rate, and nonshivering thermogenesis of *Phyllotis xanthopygus* (Rodentia) in the Andes Mountains. *J. Mammal.* **80**, 742-748. doi:10.2307/1383243

Nicholls, G. and Locke, R. (1984). Thermogenic mechanisms in brown fat. *Am. Physiol. Soc.* **64**, 1-64. doi:10.1152/physrev.1984.64.1.1

Richter, M. M., Williams, C. T., Lee, T. N., Tøien, Ø., Florant, G. L., Barnes, B. M. and Buck, C. L. (2015). Thermogenic capacity at subzero temperatures: how low can a hibernator go? *Physiol. Biochem. Zool.* **88**, 81-89. doi:10.1086/679591

Richter, M. M., Barnes, B. M., O'Reilly, K. M., Fenn, A. M. and Buck, C. L. (2017). The influence of androgens on hibernation phenology of free-living male arctic ground squirrels. *Horm. Behav.* **89**, 92-97. doi:10.1016/j.yhbeh.2016.12.007

Speakman, J. R. (2013). Measuring energy metabolism in the mouse – theoretical, practical, and analytical considerations. *Front. Physiol.* **4**, 34. doi:10.3389/fphys.2013.00034

Taylor-Burt, K. R., Monroy, J., Pace, C., Lindstedt, S. and Nishikawa, K. C. (2015). Shiver me titin! Elucidating titin's role in shivering thermogenesis. *J. Exp. Biol.* **218**, 694-702. doi:10.1242/jeb.111849

Townsend, K. and Tseng, Y.-H. (2014). Brown fat fuel utilization and thermogenesis. *Trends Endocrinol. Metab.* **25**, 168-177. doi:10.1016/j.tem.2013.12.004

Van Sant, M. J. and Hammond, K. A. (2008). Contribution of shivering and nonshivering thermogenesis to thermogenic capacity for the deer mouse (*Peromyscus maniculatus*). *Physiol. Biochem. Zool.* **81**, 605-611. doi:10.1086/588175

Verdonschot, J. A. J., Hazebroek, M. R., Derks, K. W. J., Barandiarán Aizpurua, A., Merken, J. J., Wang, P. and Heymans, S. R. B. (2018). Titin cardiomyopathy leads to altered mitochondrial energetics, increased fibrosis and long-term life-threatening arrhythmias. *Eur. Heart J.* **39**, 864-873. doi:10.1093/eurheartj/ehx808

Wunder, B. A. and Gettinger, R. D. (1996). Effects of body mass and temperature acclimation on the nonshivering thermogenic response of small mammals. In *Adaptations to the Cold: Tenth International Hibernation Symposium* (ed. F. Geiser, A. J. Hulbert and S. C. Nicol), pp. 131-139. Armindale: University of New England Press.

Yen, T. T., Fuller, R. W. and Pearson, D. V. (1974). The response of "obese" (ob/ob) and "diabetic" (db/db) mice to treatments that influence body temperature. *Comp. Biochem. Physiol. A Physiol.* **49**, 377-385. doi:10.1016/0300-9629(74)90128-5